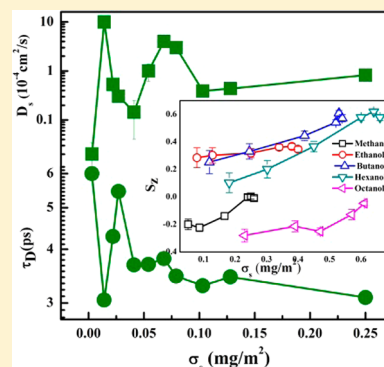


Structure and Dynamics of *n*-Alkanol Monolayers on a Mica Surface

Debdip Bhandary, Sandip Khan, and Jayant K. Singh*

Department of Chemical Engineering, Indian Institute of Technology Kanpur, Kanpur 208016, India

ABSTRACT: All-atom molecular dynamics simulations are conducted to understand the structural and dynamical behavior of self-assembled monolayer of *n*-alkanols on a mica surface. In particular, we report the effect of increasing carbon chain length (C_1 – C_{10}) on the self-assembly, surface diffusion, and preferential tilting of *n*-alkanol monolayer, for monolayer surface coverage ranging from 6×10^{-5} to 3.54×10^{-3} mol/m². The adsorption phenomena typically follow the Langmuir adsorption isotherm. However, the maximum adsorption is observed for *n*-hexanol, and it drops with further increase in the chain length. The surface diffusion coefficient, D_s , within monolayer, is nonmonotonic in nature. The maximum value of D_s decreases with increasing carbon chain length, with an exception of methanol owing to its preferential attachment with the cage of mica due to the presence of K^+ . The behavior of D_s is clearly explained using instantaneous autocorrelation function of hydrogen bonds with the surface. Further, D_s is found to vary inversely proportional to the lifetime of hydrogen bond of alkanols with the surface. Most probable tilt angle of molecules with increasing alkyl group (C_1 , C_2 , C_4 , and C_6) is in the order $71^\circ > 38^\circ > 29^\circ > 19^\circ$. However, for octanol we observed molecules to attain a preferential tilt angle of 80° . The self-assembly behavior of lower alkanols, i.e., C_1 – C_6 is contrary to that seen for higher alkanols.



1. INTRODUCTION

The self-assembly phenomena is commonly found in numerous processes ranging from life sustaining processes like folding of proteins, formation of nucleosome, etc., to physical processes such as wetting–dewetting, lubrication, and detergency.^{1,2} Study of self-assembly have immense importance in the field of biomaterials, biomedical devices,³ biosensors,⁴ micronano-electronics,⁵ and many others. Self-assembly at the interfacial region such as for self-assembled monolayers depends on the nature of the surface. In the case of the substrate, the behavior of self-assemble monolayers depends on the nature of the substrate, whether hydrophilic or hydrophobic, and its crystallographical plane.⁶ The structure and dynamics of the monolayer determines many properties like adhesion and molecular and biological recognition.⁷ Adsorption of amphiphilic molecules such as surfactants on hydrophilic solids has been studied both experimentally as well as computationally.^{6,8–17} Surfactants are found to depend strongly on the presence of water monolayer on hydrophilic surface for governing the behavior of the surfactant.¹⁰ Kinetics of adsorption is also found to depend strongly on the type of surface. For example, the adsorption rate is higher for the cationic surfactants¹³ rather than anionic and nonionic.⁹ The general adsorption isotherm of amphiphilic molecules consists of four different regimes:¹⁰ I, adsorption increases linearly with concentration, having slope typically of one, in a log–log plot; II, higher rate of adsorption due to lateral interaction of molecules leading to surface aggregation; III, adsorption rate is slower than II; IV, adsorption isotherm reaches a plateau, which is dependent on many other factors like hydrocarbon chain length, functional group, electrolyte, and temperature.

The simplest examples of amphiphilic molecules are *n*-alkanols that are found in abundance. Because of its hydrophobic backbone, their structure and dynamics are different on different surfaces. For example, on graphite surface though the backbone of *n*-alkanols remains parallel to the surface and the headgroup remains elevated from the surface.^{11–14} Moreover, this holds for other groups such as halides and COOH.¹¹ However, on hydrophilic surfaces the alkanols form tilted structure, which also depends on the substrate and drying time.^{12,16} This ordering and structure is also observed in the case of a mixture of amphiphilic molecules.⁸ However, molecules with the hydrophobic backbone, such as *n*-alkanes, form a highly ordered monolayer on surfaces like graphite¹⁷ and silica.¹⁸ The ordering is dependent on the density of the molecules.¹⁹ It has been observed that on graphite surface the backbone of alkanes remains parallel to the surface; whereas on silica surface it can bind to the surface leading to a tilted structure.¹⁸ Higher alkanes, on graphite surface, lay itself on the surface to accommodate a larger number of tails. On hydrophilic surfaces, like mica, alkanols form tilted monolayer structures, which have been predicted from the AFM images, it was concluded that the tilting increases with an increase in chain length.¹⁵ However, this is yet to be verified from other approaches such as molecular simulation or using recent experimental techniques. Recently, Cheng et al.²⁰ demonstrated using molecular dynamics that alkanols can form clusters on mica surface, in the presence of moisture, which is observed for the case of ethanol. Such

Received: December 11, 2013

Revised: March 6, 2014

Published: March 10, 2014

Table 1. Force Field Parameters for *n*-Alkanols and Mica Surface

<i>n</i> -alkanols								
nonbonded parameters					bond parameters			
atom	σ_i (Å)	ϵ_i (K)	q_i (e)		bond	k_s (kcal/mol·Å ²)	r_0 (Å)	
C (H ₃)	3.5	33.2124	-0.18		CT-CT	268	1.529	
C(H ₂)	3.5	33.2124	-0.12		HC-CT	340	1.09	
C	3.5	33.2124	0.145		CT-OH	320	1.41	
O	3.12	85.5472	-0.683		HO-H	553	0.945	
HC	2.5	15.0965	0.06					
HO	0	0	0.418					
dihedral parameters					angle parameters			
dihedral	K_1	K_2	K_3	K_4	angle	k_b (kcal/mol·rad ²)	θ_0 (deg)	
H-C-C-H	0.00	0.00	0.318	0	HC-CT-HC	33.0	107.8	
H-C-C-C	0.00	0.00	0.366	0	HC-CT-CT	37.5	110.7	
C-C-C-C	1.74	-0.157	0.279	0	CT-CT-CT	58.5	112.7	
H-C-O-H	0.00	0.00	0.45	0	HC-CT-OH	35.0	109.5	
C-C-O-H	-0.356	-0.174	0.492	0	CT-CT-OH	50.0	109.5	
H-C-C-O	0.00	0.00	0.468	0	CT-OH-HO	55.0	108.5	
C-C-C-O	1.711	-0.50	0.663	0				
mica surface nonbonded parameters								
atom		σ (Å)			ϵ (kcal/mol)		q_i (e)	
K		3.38542			0.20		1.000	
Si _{surface}		3.56359			0.05		1.100	
Al _{surface}		3.74178			0.05		0.800	
Al _{octahedral}		3.74178			0.05		1.450	
O _{surface}		3.11815			0.025		-0.550	
O _{apical}		3.11815			0.025		-0.758	
O _{hydroxyl}		3.11815			0.025		-0.683	
H _{hydroxyl}		0.97829			0.013		+0.200	

clusters are found to occur above a certain relative humidity for ethanol, which is mainly due to the role of hydrogen bonding in the adsorption.²⁰

Surface diffusion of the molecules in the monolayer plays an important role in many kinetic processes such as chemical reactions, catalysis, and crystal growth and is responsible for wetting–dewetting of a surface.²¹ On a Ag surface, it is seen that the diffusion of water in monolayer increases with an increase in surface coverage; whereas on a Pb surface the diffusion shows Λ -shaped variation.²¹ Park et al.²² has also reported that the surface diffusivity of water in monolayer on graphite also increases up to a critical coverage, and further increase in the surface coverage leads to a decrease in diffusivity. On a graphite surface, diffusion of *n*-alkanes in the monolayer also exhibits Λ -shaped anomaly. The larger alkanes diffuse faster in the case of lower coverage. On the contrary, smaller alkanes diffuse faster in the case of higher coverage.²³ Though in earlier works structural aspects of the SAM of *n*-alkanols have been studied, the surface diffusion behavior with increasing alkyl group is not known on hydrophobic or hydrophilic surface. Hence, in this work we use all-atom molecular dynamics simulation to address systematically the self-assembly behavior of *n*-alkanols. In particular, we address the surface diffusion behavior of methanol, ethanol, butanol, hexanol, octanol, and 1-decanol on a mica surface in order to understand the surface diffusion nature with increasing alkyl group. Notably, in this work, we observed that the orientations of the alkanol molecules on mica surface are contradictory to the proposed structure of Wang et al. based on AFM images.¹⁵ More importantly, we found that surface diffusion behavior of

n-alkanol monolayer is nonmonotonic in nature with surface monolayer coverage. We address the behavior by means of lifetime of hydrogen bonding of alkanol molecules on the surface. We found a clear correlation of surface diffusion with the size of the alkyl group. Structural behavior of the self-assembled monolayers of *n*-alkanols is analyzed using radial distribution function and density and orientation profiles. Adsorption isotherms generated for different concentration are being analyzed in order to gauge the process of the adsorption on the substrate and are found to follow Langmuir isotherm behavior.

2. MODELS AND METHODOLOGY

In this work we have used a fully flexible atomistic detailed model of mica, developed by Heinz et al.,²⁴ and *n*-alkanol.²⁵ The nonbonded interactions between the mica surface and alkanol molecules and between alkanol molecules are described by eq 1. The bond stretching and bending are described by using harmonic potentials as in eq 2. The dihedral interactions are calculated using OPLS-AA²⁵ force field (eq 3).

$$U_{\text{nonbond}} = 4\epsilon_{ij} \left[\left(\frac{\sigma_{ij}}{r} \right)^{12} - \left(\frac{\sigma_{ij}}{r} \right)^6 \right] + \frac{q_i q_j}{4\pi\epsilon_0 r_{ij}} \quad (1)$$

$$U_{\text{str}} = \frac{1}{2} k_s (r - r_0)^2; \quad U_{\text{bend}} = \frac{1}{2} k_b (\theta - \theta_0)^2 \quad (2)$$

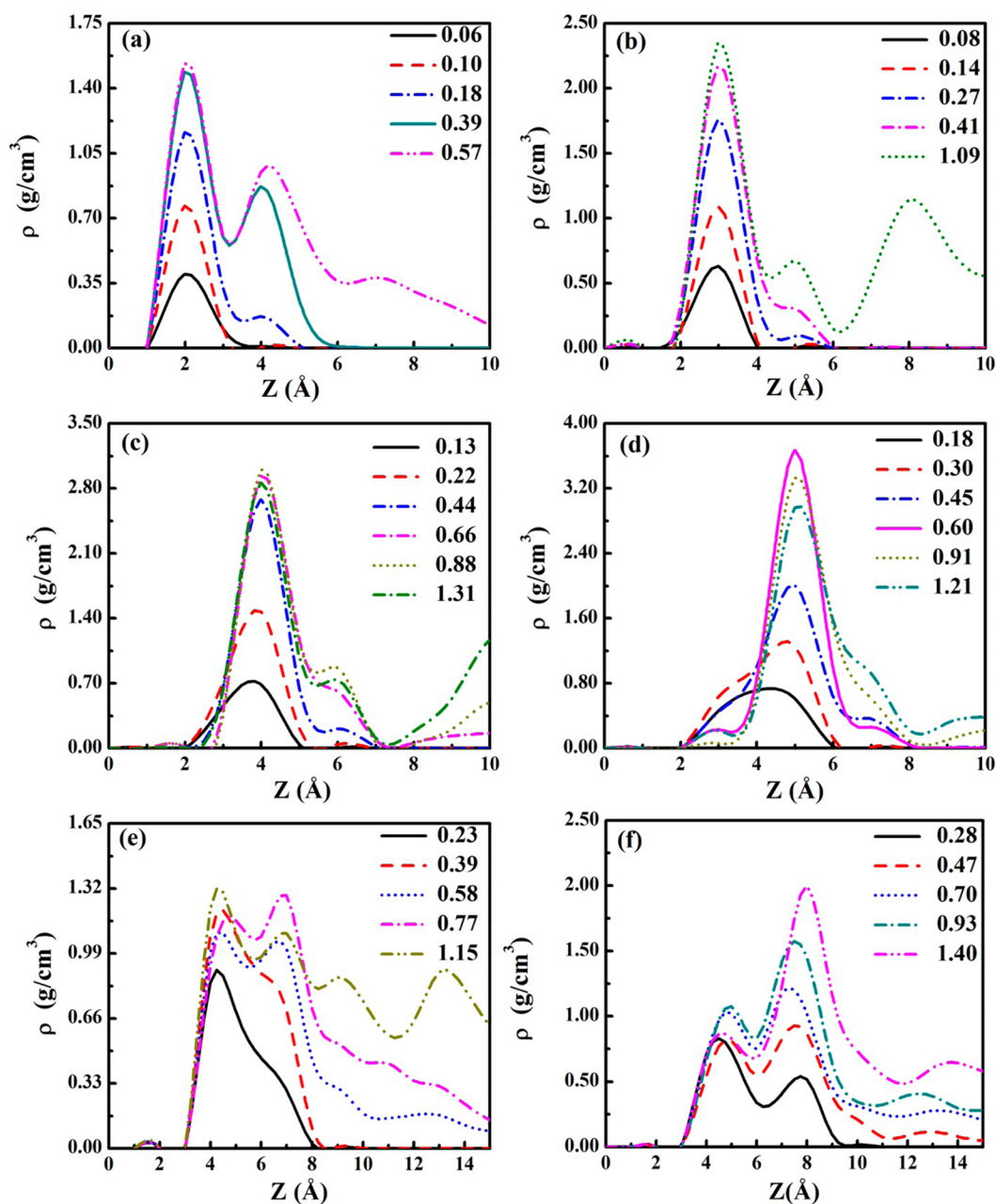


Figure 1. Local density profile (ρ) of different n -alkanols as a function of distance (Z) perpendicular to the mica surface, at different total surface coverage of methanol (a), ethanol (b), butanol (c), hexanol (d), octanol (e), and decanol (f).

$$\begin{aligned}
 U_{\text{torsion}} = & \frac{1}{2}K_1[1 + \cos(\phi)] + \frac{1}{2}K_2[1 - \cos(2\phi)] \\
 & + \frac{1}{2}K_3[1 + \cos(3\phi)] + \frac{1}{2}K_4[1 - \cos(4\phi)]
 \end{aligned}
 \quad (3)$$

Nonbonded and bonded interactions for alkanols and mica surface used in this work are described in Table 1. The fluid surface interactions are calculated using Lorentz–Berthelot geometric mixing rule.

Orientation of the molecules in the monolayer is calculated in terms of angle between axis perpendicular to the surface and end-to-end vector, which is designated by the vector connecting the end carbon atom to the oxygen atom. The orientation or ordering of alkanols is determined based on the tilt or orientational order parameter, which is given by

$$S_z = \frac{1}{2N_m} \left\langle \sum_{i=1}^{N_m} (3 \cos^2 \theta_i - 1) \right\rangle
 \quad (4)$$

where θ_i is the smallest moment of inertia axis of molecules and N_m is the number of molecules.

Hydrogen bonding between the surface and the alkanol molecules is determined by the fulfillment of the following three geometric criteria:²⁶ $r_{\text{O}_s\text{-O}_A} < 3.5 \text{ \AA}$, $r_{\text{O}_s\text{-H}} < 2.5 \text{ \AA}$, and $\theta_{\text{O}_s\text{-O}_A\text{-H}} \leq 30^\circ$ where $r_{\text{O}_s\text{-O}_A}$ is the distance between the surface oxygen atom and oxygen atom of alkanol molecule, $r_{\text{O}_s\text{-H}}$ is the distance between the hydrogen atom attached to the oxygen atom of alkanols and the surface oxygen atom, and $\theta_{\text{O}_s\text{-O}_A\text{-H}}$ is the angle between the vector connecting two oxygen atoms and the vector connecting the OH group. The lifetime of the

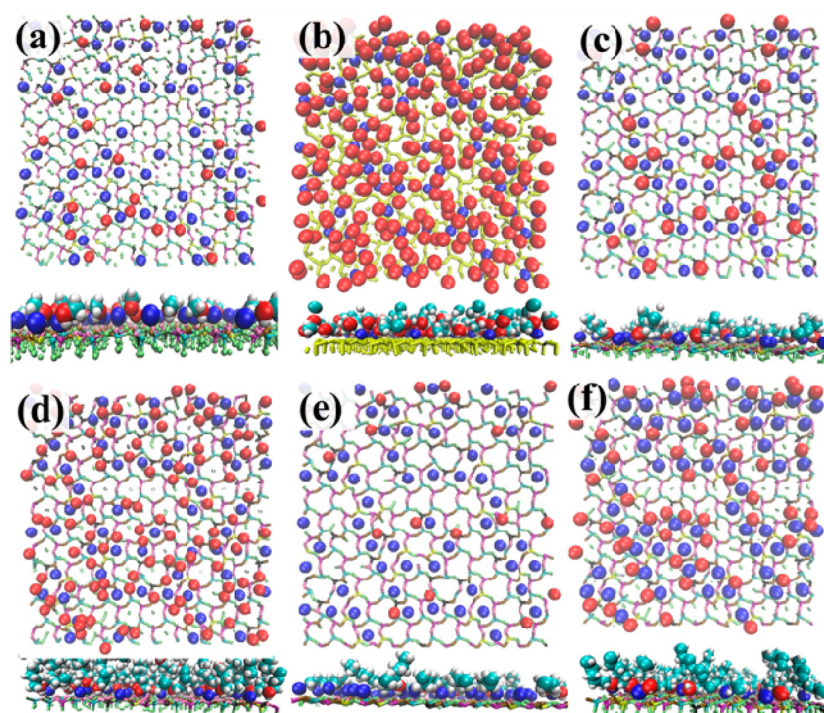


Figure 2. Snapshots of alkanol molecules at different monolayer surface coverage. Red spheres represent oxygen atoms, green spheres represent carbon atoms, blue spheres represent potassium ions on the mica surface, and white ones represent hydrogen atoms. Wire frame structure is for the mica surface. Layers on the top of the monolayer are removed for clarity. Each panel contains the top view (top image contains oxygen of alkanols, and potassium ions on the wire frame are shown for the clarity) and side view (bottom image shows the alignment of the molecules). Panels a and b represent the snapshot of methanol monolayer on the mica surface at lower (0.05 mg/m^2) and higher (0.26 mg/m^2) monolayer surface coverage, respectively. Panels c and d represent similarly *n*-butanol at lower (0.12 mg/m^2) and higher (0.54 mg/m^2) monolayer surface coverage, respectively. Panels f and e represent *n*-octanol molecules on the mica surface at higher (0.43 mg/m^2) and lower (0.13 mg/m^2) monolayer surface coverage, respectively.

hydrogen bond of the alkanols with the surface, i.e., the lifetime of the jump of the molecules from an adsorbed site, is defined by an instantaneous autocorrelation function, C_{HB}

$$C_{\text{HB}}(t) = \langle h(t)h(0) \rangle / \langle h \rangle = \exp(-t/\tau_{\text{D}}) \quad (5)$$

where $h(t) = 1$ if alkanol molecules remain bonded with the surface oxygen atom at time t and τ_{D} is the lifetime of the hydrogen bonds.

3. SIMULATION DETAILS

The substrate consists of two mica sheets, each with lateral dimension of $5.4 \times 5.1 \text{ nm}^2$. Periodic boundary conditions are applied in all three directions. We have kept the *Z*-height of the simulation box sufficiently large enough (225 \AA) to prevent the effect of the opposite side of the mica surface. The alkanol molecules are inserted randomly near the surface. The number of molecules varies depending on the surface coverage. In this work, the maximum numbers of molecules are 400 for methanol and ethanol, 300 for butanol and hexanol, and 200 for octanol and decanol. The randomly inserted molecules are allowed to equilibrate and form self-assembled layers. We have also checked with incremental addition to the configuration of a previous coverage simulation to generate initial configuration for higher coverage simulation. We found that it does not affect the final structure and dynamic of the adsorbed *n*-alkanol layers. Particle–particle particle–mesh (PPPM) technique is applied for the calculation of long-range electrostatic forces. The cut off distance is 15 \AA . Nosé–Hoover thermostat and Berendsen barostat are used to maintain temperature of the system at 300

K and pressure at 1 atm, respectively. The integration time of 1 fs is used in this work. All simulations are performed using LAMMPS²⁷ molecular dynamics package.

Each simulation is equilibrated for 1.5 ns in the NPT ensemble. Subsequently, study of the structure and dynamical properties of alkanols on the mica surface is performed in the canonical ensemble for 2.5 ns. The mean squared displacement is block averaged during the production run, with three blocks of 800 ps. The diffusivity coefficient is calculated using the Einstein equation for the 2D case.²⁰ The time average positions of atoms are taken for the calculation of surface density, diffusivity, orientation profile, and in-plane radial distribution function. The monolayer layer coverage, σ_{s} , is defined as the monolayer mass per unit surface area in mg/m^2 .

4. RESULTS AND DISCUSSION

We start with the density profile based on the center of mass of *n*-alcohols of variable chain length as shown in Figure 1, for different total surface coverage, which is defined as total mass of the alkanols per unit surface area. Alkanols, due to strong electrostatic attraction and van der Waal's attraction, adsorb strongly on the mica surface. At a low value of total surface coverage only a single layer on the surface is seen, as indicated by Figure 1a for methanol. With increasing concentration second or higher layers appear. For example, a second peak is visible for total surface coverage of 0.18 mg/m^2 and above, for methanol. Similarly, formation of second layer is also visible for ethanol (Figure 1b) at 0.27 mg/m^2 , for butanol (Figure 1c) at 0.44 mg/m^2 , and for hexanol (Figure 1d) at 0.60 mg/m^2 . The

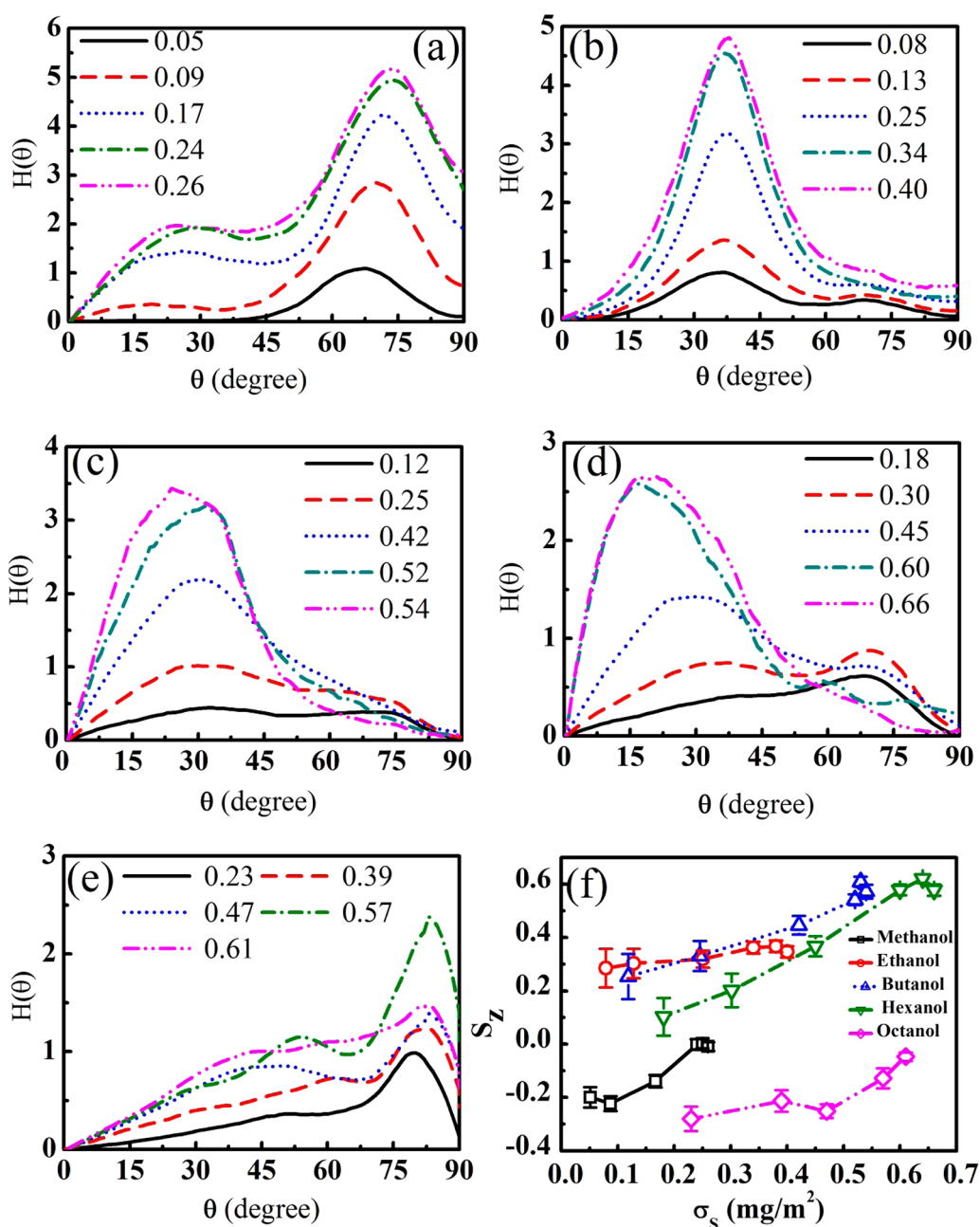


Figure 3. Panels a–e represent histograms of the tilt angle, H , for methanol, ethanol, butanol, hexanol, and octanol, respectively, within the monolayer at different monolayer surface coverage. Panel f shows the variation of tilt or orientational order parameter, S_z , of alkanols with the monolayer surface coverage, σ_s .

first peak in the density profile represents the first layer followed by saturation values corresponding to the bulk value, which at a low coverage is close to zero. Interestingly, in the ethanol density profile a hump appears at higher coverage that is visibly evident for the case of 1.09 mg/m². The hump is followed by another peak indicating clearly the bilayer. As the chain length increases, the hump gradually gets suppressed. The peak of the first layer is slightly shifted toward the right with increasing alkyl group chain length until hexanol. Subsequently, the typical behavior of the density profile is not seen. Instead, we observed a split peak for the case of octanol, which indicates that self-assembly behavior is now different, and monolayer formation is not favorable, as opposed to the case of lower alkanes. This is clearly evident for the case of 1-decanol, as in

Figure 1f, which displays maximum density away for the monolayer region. With increase in total surface coverage, there is no significant change in the peak corresponding to the monolayer region, in contrast to the case of lower alkanols. This indicates that adsorption behavior of *n*-octanol and particularly 1-decanol is more of agglomeration rather than layering. Hence, self-assembly behavior of alkanols on the mica surface depends strongly upon the backbone of the alkanols.

Surface adsorption of alkanols is due to the strong electrostatic and van der Waal's attraction between the alkanols and the mica. The alkanol molecules spread themselves on the surface that facilitates monolayer formation. An increase in number of molecules, beyond a critical value, which varies with alkyl chain length, initiates the formation of the second layer. In

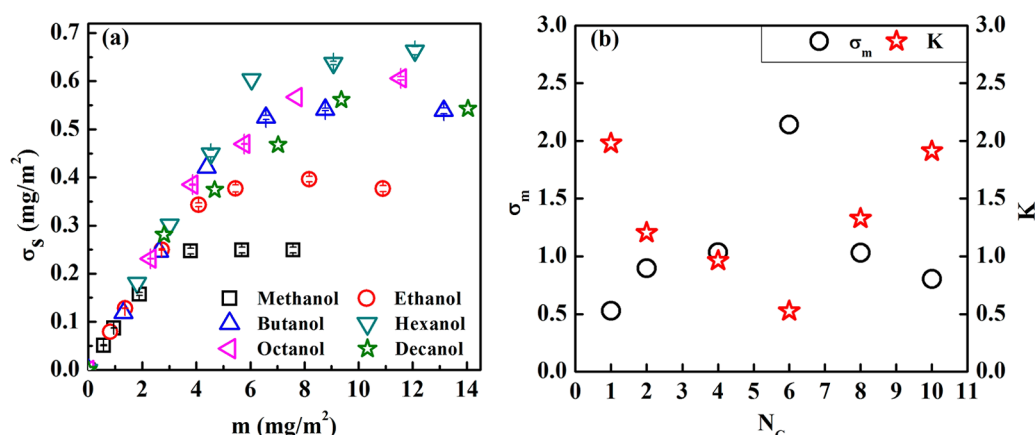


Figure 4. Adsorption isotherm (panel a) of alkanols on the mica surface at 298 K and 1 atm pressure. The x -axis represents the total surface coverage; whereas the y -axis represents the monolayer surface coverage σ_s . Panel b shows the maximum adsorption (left axis) of alkanols within monolayer and variation of Langmuir equilibrium constant, K (right axis), for different alkanols.

the density profile (Figure 1), each crest and trough represents layering of alkanols up to n layers. The first trough at the left is considered as the thickness of the monolayer. The thickness of the monolayer is 3.5 ± 0.2 Å for methanol, which is less than the thickness of monolayer (4.5 Å) measured using AFM by Wang et al.¹⁵ Similarly, the thickness of monolayer of other alkanols is also calculated, and the thicknesses are as follows: ethanol 4.5 ± 0.3 Å, butanol 5.5 ± 0.1 Å, hexanol 8.2 ± 0.1 Å, and octanol 5.6 ± 0.3 Å. However, in case of decanol no clear monolayer is formed; instead, agglomeration is seen. The lower alkanols, i.e., methanol and ethanol, due to their small backbone and tendency to form hydrogen bonds, tend to form an extended monolayer, which is not a separate layer rather a layer formed by molecules that remained hydrogen bonded with molecules of monolayer, and compete with each other in order to find a place in the monolayer. Thus, the higher density is obtained at the trough of the density profile for lower alkanols than the higher alkanols.

At lower monolayer coverage (σ_s) the alkanol molecules remain distributed and do have space to move around as clearly seen in Figure 2a; whereas with an increase in density, packed structure does not provide enough space for movement (see Figure 2b top view). Hence, hopping of molecules is observed frequently at lower coverage, particularly for smaller alkanols, that is rarely observed at higher coverage. At higher coverage methanol molecules remain tilted toward the surface even for higher σ_s ; whereas butanol molecules (Figure 2c side view) tend to remain more perpendicular to the surface at higher σ_s (Figure 2d side view) than at lower σ_s (Figure 2c side view). In the case of octanol, due to the larger backbone, molecules tend to remain aligned to the surface at lower σ_s (Figure 2f side view). A layer of variable thickness is observed for octanol, at higher σ_s (Figure 2e).

The effect of alkyl chain length or backbone is clearly observed in the orientation profile. Figure 3 presents orientation profiles of n -alkanols. With increase in chain length, the monolayer becomes more perpendicular to the surface. For methanol, tilt angle slightly changes from 67° at 0.05 g/cm³ to 73° at 0.26 g/cm³. Methanol molecules display another orientation with a tilt angle at around 20° , though not predominant; however, with increasing concentration it is accentuated. Though methanol molecules have a preference of higher tilt angle, it decreases with increasing alkyl chain length as seen for ethanol, butanol, and hexanol with tilt angles 40° ,

30° , and 20° , respectively. The single peak in the orientation profile indicates strongly that almost all molecules tend to orient along a single tilt angle, though it is more prominent at higher monolayer coverage. At lower monolayer coverage, there is no visible strong peak as seen for butanol or possibly more than one preferential orientation as seen for hexanol. It should be noted that for butanol and hexanol, as the concentration increases the orientation becomes more perpendicular to the surface.

With an increase in the alkyl group to octanol, a remarkable change is observed. The tilt angle jumps from 20° for hexanol to 80° for octanol. At a lower concentration one clear peak is observed for the octanol systems, which slightly reduces with an increase in concentration. At a higher concentration, the second peak starts emerging at around tilt angle 53° . However, the orientational behavior of octanol is found to be similar to that of methanol. Layering of octanol molecules on the surface is also evident from the density profile as the monolayer height is lower than that of hexanol. From the tilt order parameter analysis, Figure 3f, it also reflects how the ordering of alkanols within the monolayer changes with the variation of monolayer coverage. As the coverage increases, the tilt order parameter increases, which helps to conclude that the ordering of the monolayer increases with an increase in concentration. Similar behavior is also observed in the case of tilting of hexane on graphite surface.²⁸ We note Wang et al.¹⁵ predicted that the small alkanols remain perpendicular to the mica surface, and as the chain length increases the monolayer increasingly tilts toward the surface, which is in contrast to our results. We attribute the disagreement to the difficulty associated with interpreting the AFM images in the experiments.

Figure 4a presents the monolayer adsorption isotherm of n -alkanol on mica surface at a temperature 300 K and pressure 1 atm. The monolayer adsorption of n -alkanols on mica surface follows the Langmuir isotherm behavior, akin to that seen for water²⁹ and ethanol²⁰ on mica surface. The adsorption isotherm of amphiphilic molecules on different surfaces consists of four different regions, as mentioned earlier. Since in this study, our focus is on the adsorption of the monolayer, thus the isotherms presented in Figure 4a do not consist of all the regions. As the number of molecules increases, the isotherm, in log–log scale, increases linearly with a slope of one. Further increase in the coverage leads to decrease in slope, and finally reaches a plateau. Subsequent increase in the number of

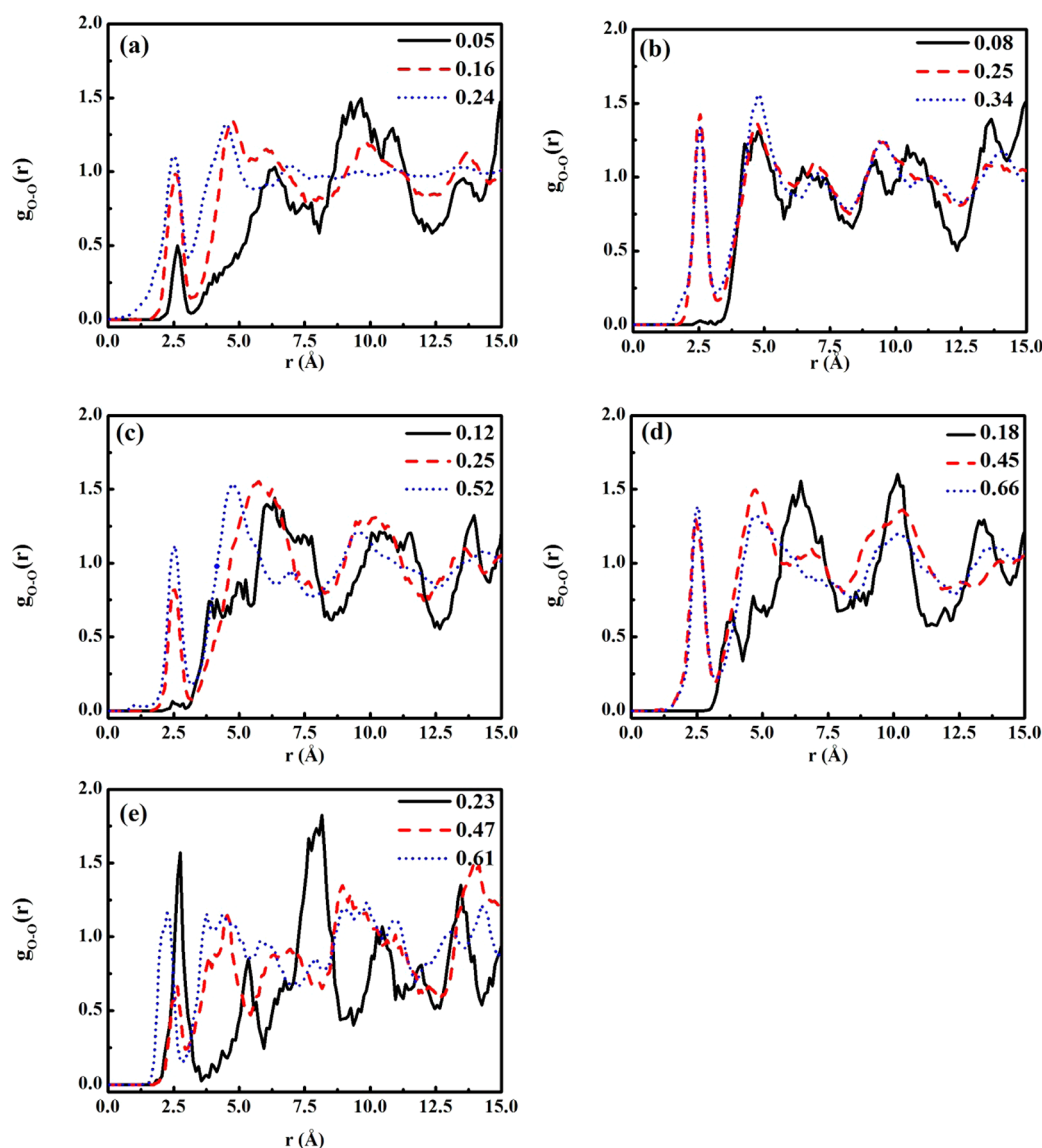


Figure 5. In-plane radial distribution function of the hydroxyl oxygen within the monolayer formed on the mica surface for different monolayer surface coverage. Panels a–e represent the radial distribution function of methanol, ethanol, butanol, hexanol, and octanol, respectively.

molecules will facilitate the formation of the second layer. In order to understand the nature of the isotherm, we fit the data to the Langmuir isotherm, which is defined as

$$\sigma_s = \sigma_m \frac{Kc}{1 + Kc} \quad (6)$$

where σ_s and σ_m represent the amount adsorbed and the maximum amount of adsorption on the surface, respectively, K is the Langmuir equilibrium constant, and the total surface coverage is denoted by c . The adsorption isotherms are found to fit very well by eq 6 indicating strongly that the adsorption of n -alkanols on the mica surface follows the Langmuir isotherm. Figure 4b shows σ_m and K as a function of the number of carbons, N_c , in n -alkanols. The maximum adsorption increases with an increase in N_c until C_6 . In the analysis of adsorption of higher alkanols, e.g., octanol and decanol, we found that the maximum adsorption is less than that of hexanol. The maximum at C_6 is well supported by the orientational behavior, which also peaks at C_6 indicating the maximum amount

adsorbed for hexanol due to the best packing geometry (see Figure 3d).

In order to quantify the self-assembly behavior of n -alkanols, we also looked into the radial distribution functions of different alkanols within the monolayer at different monolayer coverage, as shown in Figure 5. Since the alkanols are bound to surface via $-\text{OH}$ group, hence the in-plane radial distribution function (RDF) is calculated for O–O pair. At a lower coverage, for all the alkanols, the RDF is having strong oscillation at uniform distance. RDF with strong oscillation is characteristic of states with frozen molecules, which is also evident from the low diffusivity values. Thus, at lower monolayer coverage, due to the strong attraction with the surface, the structure is relative long-ranged;³⁰ whereas at a higher coverage the oscillation decays and the behavior is more liquid-like.

However, for methanol (see Figure 5a) the first peak at 2.5 Å has a value less than one, indicating a depletion behavior at a very low concentration. This perhaps could be because of low cohesive forces compared to adhesive, which binds the methanol molecules to the surface. The subsequent peak

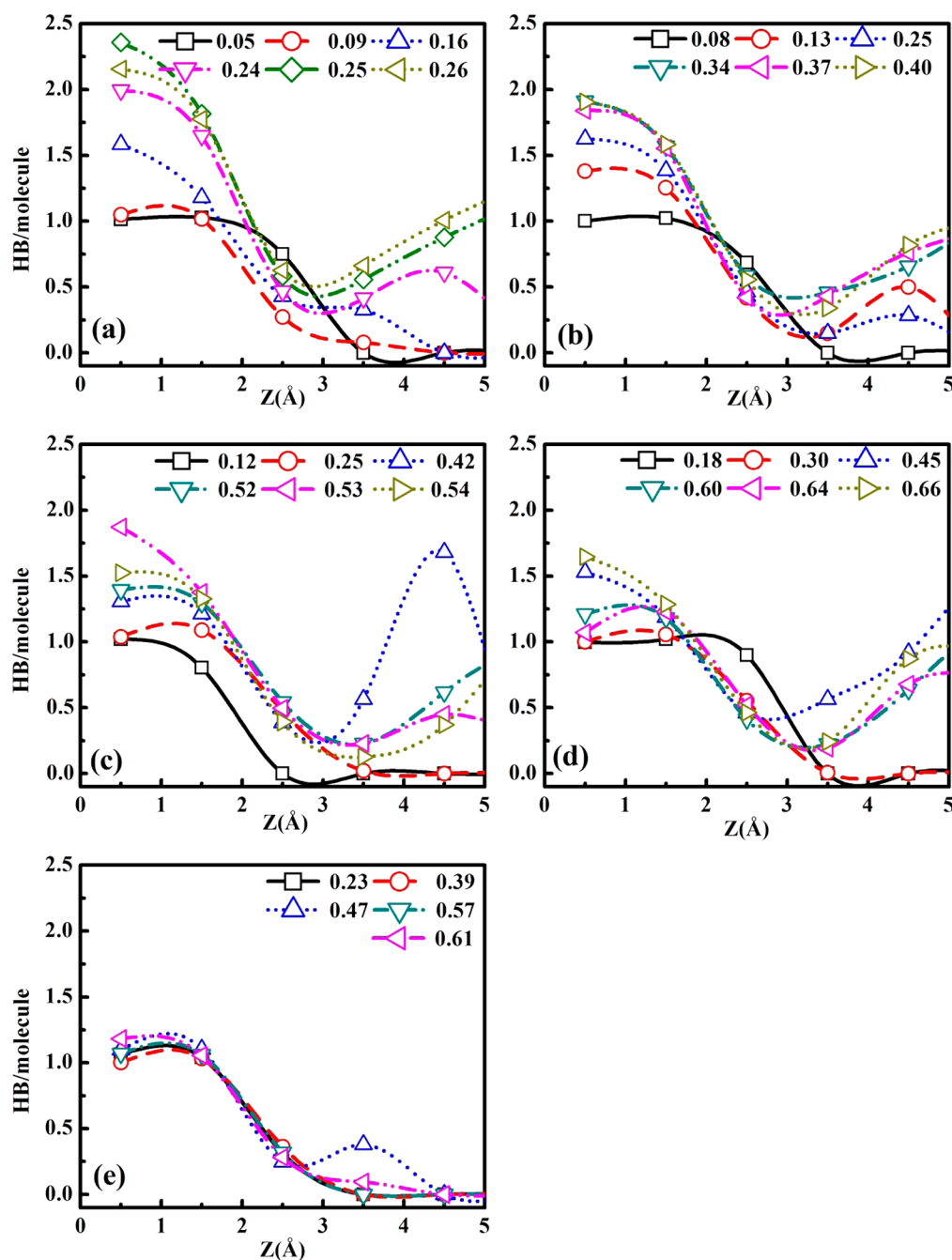


Figure 6. Hydrogen bond (HB) per molecule for methanol (a), ethanol (b), butanol (c), hexanol (d), and octanol (e) as a function of distance, Z , perpendicular to the mica surface. Symbols represent different monolayer surface coverage in mg/m^2 .

value increases, which implies that at this range of monolayer coverage the effect of surface is less, and intermolecular interactions start affecting the nature of the monolayer structure. This is also indicated by the increase in the diffusivity value, as shown later in the article. As the monolayer coverage of methanol increases, the first peak value increase and goes beyond 1, thus creating a coordination shell. In the case of the ethanol, at a lower concentration, $0.08 \text{ mg}/\text{m}^2$, the first peak occurs at 4.9 Å . However, at a higher surface coverage the first peak shifts to the earlier value at 2.5 Å . It is evident that the first peak at 2.5 Å is suppressed successfully at $0.08 \text{ mg}/\text{m}^2$, which appears only at higher concentrations. Similar behavior is seen for higher alkanols. The exception is octanol, which has a peak at 2.5 Å even at the lowest concentration and that too was

accentuated indicating a different self-assembly behavior due to its strong backbone effect on the structure of the monolayer. At lower surface coverage, the movement of the molecules is limited due to strong binding between the K^+ ions and the OH group of alkanols, which is the main reason behind the suppression of the peak at 2.5 Å of RDF. An increase in the concentration makes the intermolecular interaction strong enough to overcome the surface–OH attraction that enhances the mobility of the alkanols. This allows the molecules to come closer at 2.5 Å as seen for higher surface coverage. The effect is similar for higher alkanols where this behavior is seen at a much lower number of molecules; that is clearly evident for the case octanol, where it is seen at $0.23 \text{ mg}/\text{m}^2$, indicated by the larger peak of the first coordination shell.

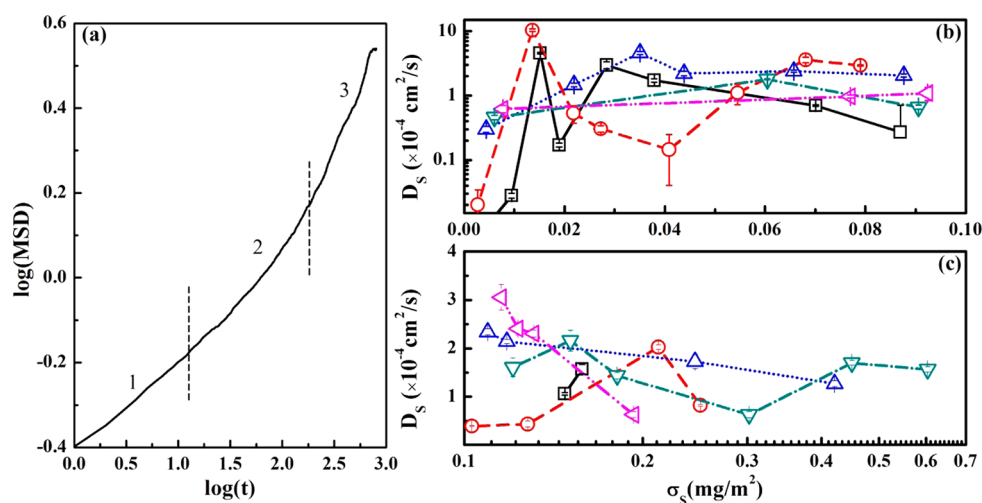


Figure 7. (a) Typical mean square displacement (MSD) plot of *n*-butanol as a function of time, in a log–log scale. Regions 1, 2, and 3 represent different slopes of the diffusivity plot. (b) Diffusivity of different alkanols on a mica surface, D_s , at lower monolayer surface coverage ($\sigma_s < 0.1 \text{ mg/m}^2$). (c) Variation of diffusion coefficient at higher monolayer surface coverage ($\sigma_s > 0.1 \text{ mg/m}^2$). The symbols square, circle, up-triangle, down-triangle, and left-triangle represent methanol, ethanol, butanol, hexanol, and octanol, respectively.

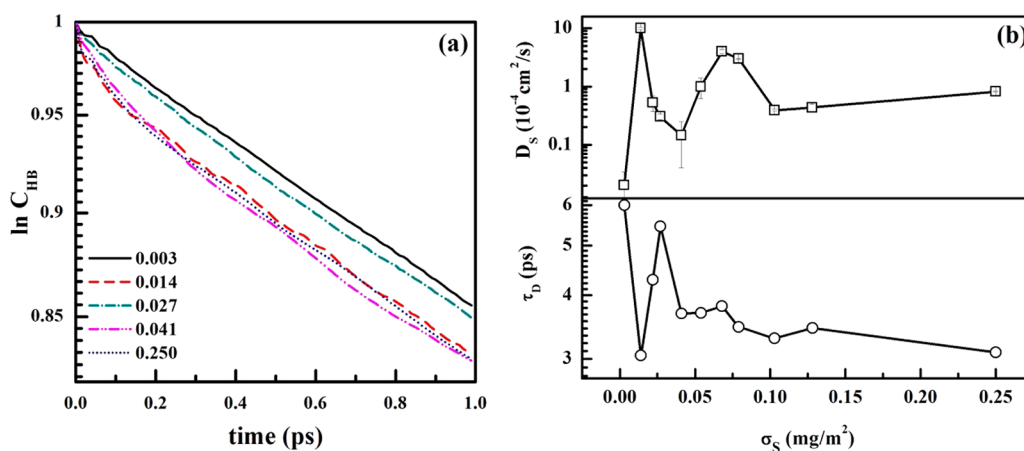


Figure 8. (a) Instantaneous autocorrelation function of hydrogen bond of ethanol with the surface as a function of time. (b) Variation of lifetime of hydrogen bond and surface diffusion coefficient with monolayer surface coverage.

The oxygen atom on the exterior of the mica surface and presence of K^+ ion also create a favorable environment for the O–H group of *n*-alkanols to get bonded to the surface via the formation of hydrogen bonding. Thus, hydrogen bonding plays an important role in the structure and dynamics of the monolayer. The molecules are arrested into the cage of mica surfaces, and hence, strong hydrogen bonding as well as strong electrostatic attraction between K^+ ions and –OH group does not allow it to move freely. In case of methanol, Figure 6a, at concentration of 0.05 mg/m^2 , the hydrogen bond (HB) per molecule of *n*-alkanol is equal to unity at $z = 0$, which is also seen for ethanol, butanol, hexanol, and octanol (see Figure 6b–e, respectively). As seen in Figures 2 and 5, the molecules are far apart at lower monolayer coverage, 0.05 mg/m^2 ; hence, the hydrogen bonds are due to surface bonding. However, an increase in surface coverage leads to sharing of molecules by the sites, indicated by an increase in HB per molecule. This ability of *n*-alkanols on mica surface gradually decreases as the chain length increases, and in the case of octanol, hydrogen bonding is always unity even at higher monolayer coverage.

In order to understand the nature of diffusion and the variation of diffusion coefficients with the surface concen-

tration, we resort to the mean-squared displacement (MSD) calculation. Figure 7a shows the typical MSD of *n*-alkanol on the mica surface. The slope of the regime 1, 2, and 3 are ~ 0.2 , ~ 0.5 , and ~ 1.0 , respectively. Diffusion coefficients are calculated based on the average slope of regime 3 over 0.5 ns. The calculated value of the self-diffusion coefficient is found to be of the same order as reported by Bo et al. for the case study of ethanol on mica surface.¹⁴

In earlier studies, diffusion of water shows Λ -shaped variation with surface coverage on hydrophilic surface like lead, whereas it increases monotonously on Ag surface, which is also hydrophilic in nature.²¹ On a graphene surface, formation of structured monolayer and Λ -shaped variation in diffusivity with the surface coverage has been observed as well as for alkanes on graphite surface.²² The behavior of diffusivity of an amphiphilic-polar molecule within the monolayer, on a hydrophilic surface, mica, with surface concentration is different from the behavior mentioned in earlier studies.^{14,21–23} The surface diffusion coefficient, D_s , of *n*-alkanols on a mica surface is found to be highly dependent on the nature of the backbone of the alkanols. Figure 7b shows the appearance of multiple peaks for different alkanols with increasing monolayer coverage. The diffusion

coefficient oscillates with the monolayer coverage, which eventually subsides at a monolayer coverage of 0.2 mg/m^2 . It is also observed that the higher alkanols diffuse faster than the lower ones at lower surface coverage, whereas the lower ones are faster at higher surface coverage, which is found to be similar in the case of diffusion of alkanes on a graphite surface.²³

To this end, we evaluate the lifetime of the hydrogen bond with the surface in order to understand its relationship with the surface diffusion as per eq 5. Figure 8a shows the relationship between the diffusivity and the hydrogen bond lifetime; whereas Figure 8b, for the case of ethanol, shows the nature of the decay of C_{HB} with time and its variation of slope as the surface concentration changes. As the slope of the decay curve increases, the lifetime of HB, τ_{D} , decreases. In this case, we have found that τ_{D} for the hydrogen bonds of different alkanols with the surface is of the order of 1–10 ps. On comparing with the diffusivity at a certain surface concentration it is found that τ_{D} and diffusivity are inversely proportional. Hence, it can be concluded that the diffusion of *n*-alkanol is inversely proportional to the lifetime of hydrogen bonds formed between the surface and the alkanols molecules.

5. CONCLUSIONS

The surface adsorption and diffusion of simpler amphiphilic molecules, *n*-alkanols, within the monolayer on hydrophilic surface, mica, are studied using molecular dynamics simulations. The adsorption of alkanol on the surface to form a monolayer is dependent on the chain length of the backbone, which also holds the key in the orientation of the monolayer. Tilt angle of the monolayer decreases as the chain length of the alkanols increases up to 6, beyond which it increases with an increase in chain length. The adsorption of *n*-alkanols follows Langmuir isotherm, and the maximum adsorption within the monolayer is found to increase until hexanol, and drops as the backbone is further increased. The surface diffusion coefficient oscillates with increasing surface monolayer coverage. Hydrogen bonding with the surface by the alkanols plays an important role in the diffusion. The longer alkanols diffuses faster at lower concentration, whereas the smaller alkanols do at higher concentrations. The diffusion coefficient is found to vary inversely with the lifetime of hydrogen bonds with the surface. A similar behavior is also seen for *n*-alkanes on graphite surface where the Λ -shape behavior of the diffusion coefficient with surface coverage is attributed to the molecule–surface interactions as well as the rotational motion of the molecules.²³

AUTHOR INFORMATION

Corresponding Author

*(J.K.S.) E-mail: jayantks@iitk.ac.in.

Notes

The authors declare no competing financial interest.

ACKNOWLEDGMENTS

This work was supported by the Department of Science and Technology (DST), Government of India. Computational resources were provided by the Centre for Development and Advance Computing (CDAC) Pune, India, and HPC cluster of the Computer Center (CC), Indian Institute of Technology Kanpur.

REFERENCES

- (1) Percec, V.; Ungar, G.; Peterca, M. Self-Assembly in Action. *Science* **2006**, *313*, 55–56.
- (2) Sammalkorpi, M.; Karttunen, M.; Haataja, M. Structural Properties of Ionic Detergent Aggregates: A Large-Scale Molecular Dynamics Study of Sodium Dodecyl Sulfate. *J. Phys. Chem. B* **2007**, *111*, 11722–11733.
- (3) Riess, J. G. Fluorous Micro- and Nanophases with a Biomedical Perspective. *Tetrahedron* **2002**, *58*, 4113–4131.
- (4) Kind, M.; Wöll, C. Organic Surfaces Exposed by Self-Assembled Organothiol Monolayers: Preparation, Characterization, and Application. *Prog. Surf. Sci.* **2009**, *84*, 230–278.
- (5) Vuillaume, D. Molecular-Scale Electronics. *C. R. Phys.* **2008**, *9*, 78–94.
- (6) Núñez-rojas, E.; Domínguez, H. Computational Studies on the Behavior of Sodium Dodecyl Sulfate (SDS) at TiO₂ (Rutile)/Water Interfaces. *J. Colloid Interface Sci.* **2011**, *364*, 417–427.
- (7) Rabe, J. P.; Buchholz, S. Commensurability and Mobility in Two-Dimensional Molecular Patterns on Graphite. *Science* **1991**, *253*, 424–427.
- (8) Domínguez, H. Structure of the SDS/1-Dodecanol Surfactant Mixture on a Graphite Surface: A Computer Simulation Study. *J. Colloid Interface Sci.* **2010**, *345*, 293–301.
- (9) Paria, S.; Manohar, C.; Khilar, K. C. Adsorption of Anionic and Non-Ionic Surfactants on a Cellulosic Surface. *Colloids Surf., A* **2005**, *252*, 221.
- (10) Paria, S.; Khilar, K. C. A Review on Experimental Studies of Surfactant Adsorption at the Hydrophilic Solid-Water Interface. *Adv. Colloid Interface Sci.* **2004**, *110*, 75–95.
- (11) Claypool, C. L.; Faglioni, F.; Matzger, A. J.; Goddard, W. A., III; Lewis, N. S. Effects of Molecular Geometry on the STM Image Contrast of Methyl- and Bromo-Substituted Alkanes and Alkanols on Graphite. *J. Phys. Chem. B* **1999**, *103*, 9690–9699.
- (12) Mugele, F.; Baldelli, S.; Somorjai, G. A.; Salmeron, M. Structure of Confined Films of Chain Alcohols. *J. Phys. Chem. B* **2000**, *104*, 3140–3144.
- (13) Biswas, S. C.; Chatteraj, D. K. Kinetics of Adsorption of Cationic Surfactants at Silica–Water Interface. *J. Colloid Interface Sci.* **1998**, *205*, 12–20.
- (14) Bo, Z.; Chun-Lei, W.; Peng, X.; Hai-Ping, F. Structure and Dynamics of Ethanol Adsorbed on a Mica Surface. *Commun. Theor. Phys.* **2012**, *57*, 308–314.
- (15) Wang, L.; Song, Y.; Zhang, B.; Wang, E. Adsorption Behaviors of Methanol, Ethanol, *n*-Butanol, *n*-Hexanol and *n*-Octanol on Mica Surface Studied by Atomic Force Microscopy. *Thin Solid Films* **2004**, *458*, 197–202.
- (16) Wang, L.; Song, Y.; Wu, A.; Li, Z.; Zhang, B.; Wang, E. Study of Methanol Adsorption on Mica, Graphite and ITO Glass by Using Tapping Mode Atomic Force Microscopy. *Appl. Surf. Sci.* **2002**, *199*, 67–73.
- (17) Morishige, K.; Takami, Y.; Yokota, Y. Structures of Alkanes and Alkanols Adsorbs on Graphite in Solution: Comparison with Scanning-Tunneling-Microscopy Images. *Phys. Rev. B: Condens. Matter Mater. Phys.* **1993**, *48*, 8277–8281.
- (18) Sieval, A. B.; Hout, B. V. D.; Zuilhof, H.; Sudholter, E. J. R. Molecular Modeling of Alkyl Monolayers on the Si(111) Surface. *Langmuir* **2000**, *16*, 2987–2990.
- (19) Roth, M. W.; Kaspar, M.; Wexler, C.; Firlej, L.; Kuchta, B. Molecular Dynamics Simulations of Submonolayer Hexane and Pentane Films on Graphite. *Mol. Simul.* **2010**, *36*, 326–333.
- (20) Cheng, T.; Sun, H. Adsorption of Ethanol Vapor on Mica Surface under Different Relative Humidities: A Molecular Simulation Study. *J. Phys. Chem. C* **2012**, *116*, 16436–16446.
- (21) Park, J. H.; Aluru, N. R. Diffusion of Water Submonolayers on Hydrophobic Surfaces. *Appl. Phys. Lett.* **2008**, *93*, 253104.
- (22) Park, J. H.; Aluru, N. R. Ordering-Induced Fast Diffusion of Nanoscale Water Film on Graphene. *J. Phys. Chem. C* **2010**, *114*, 2595–2599.

- (23) Park, J. H.; Aluru, N. R. Surface Diffusion of *n*-Alkanes: Mechanism and Anomalous Behavior. *Chem. Phys. Lett.* **2007**, *447*, 310–315.
- (24) Heinz, H.; Koerner, H.; Anderson, K. L.; Vaia, R. A.; Farmer, B. L. Force Field for Mica-type Silicates and Dynamics of Octadecylammonium Chains Grafted to Montmorillonite. *Chem. Mater.* **2005**, *17*, 5658–5669.
- (25) Jorgensen, W. L.; Maxwell, D. S.; Tirado-Rives, J. Development and Testing of the OPLS All-Atom Force Field on Conformational Energetics and Properties of Organic Liquids. *J. Am. Chem. Soc.* **1996**, *118*, 11225–11236.
- (26) Chowdhuri, S.; Chandra, A. Dynamics of Halide Ion-Water Hydrogen Bonds in Aqueous Solutions: Dependence on Ion Size and Temperature. *J. Phys. Chem. B* **2006**, *110*, 9674–9680.
- (27) Plimpton, S. Fast Parallel Algorithms for Short-Range Molecular Dynamics. *J. Comput. Phys.* **1995**, *117*, 1–19.
- (28) Pint, C. L.; Roth, M. W.; Falls, C.; Wexler, C. Behavior of Hexane on Graphite at near-Monolayer Densities: Molecular Dynamics Study. *Phys. Rev. B* **2006**, *73*, 085422.
- (29) Malani, A.; Ayappa, K. G. Adsorption Isotherms of Water on Mica: Redistribution and Film Growth. *J. Phys. Chem. B* **2009**, *113*, 1058–1067.
- (30) Cui, S. T.; Cummings, P. T.; Cochran, H. D. Molecular Simulation of the Transition from Liquidlike to Solidlike Behavior in Complex Fluids Confined to Nanoscale Gaps. *J. Chem. Phys.* **2001**, *114*, 7189–7195.